Flexible Phase Synchronization for Wireless Optical Coherent Communication System With Adaptive Fractionally-Spaced Blind Equalization Combined With Adaptive Kalman Filter

ShuPeng Zhang, LiYing Tan, and Jing Ma

***Abstract*—Wireless optical coherent communication can be used as the backbone supporting technology of air-space-ground-sea-integrated network. In wireless optical coherent communication, the information can be demodulated from the carrier correctly only when the phase synchronization is accurate. Operating in different systems and diverse environments presents challenges for phase synchronization, especially lasers with different line-widths and atmospheric turbulence channels that cause scintillation and wave-front distortion. We propose a combination of adaptive fractionally-spaced blind equalization and adaptive kalman filter to realize phase synchronization under different line-widths and different scintillation and wave-front distortion. This combination which changed the limitation that the original settings of each part is not directly applicable to atmospheric channel combines spatial diversity in a natural way, jointly removes amplitude noise and phase noise more thoroughly with the optimal bandwidth, and can realize phase synchronization under time-varying conditions. The signal quality of the proposed scheme with constant parameter output can be improved 1-2dB in both mean square error (MSE) and symbol to error ratio (SER) compared to traditional equal gain combining (EGC) followed by Viterbi-Viterbi phase estimation (VVPE) and the proposed constant parameter scheme has more laser line-width options. The proposed scheme with noise parameter corrected by Autoregressive method outperforms the constant parameter scheme 1-2dB at both MSE and SER and has higher and wider line-width selections. With this design, phase synchronization can be more flexible to adapt to dynamic changes, which will be more suitable for future applications of wireless optical networks with dynamic,noisy, diverse environment.**

***Index Terms*—Adaptive Kalman filter, atmospheric turbulence, coherent communication, fractionally-spaced dual-mode blind equalization, free space optical communication.**

I. Introduction

AERIAL-spatial-terrestrial-marine integrated network is the trend, involving various terminal platforms, various relay systems and different distance routing and working environment [1]. Recently, many fundamental works have been conducted focusing on the FSO communication system in deep space [2], [3], [4], and provided fruitful results and helpful insights for future deep space communication. Wireless optical coherent communication, with its high communication rate and high sensitivity, has greater advantages in the communication rate distance product [5], and should become an important technical option and component of aerial-spatial-terrestrial-marine integrated network. However, wireless optical coherent communication requires phase synchronization to properly demodulate information [6], which is a challenge in different systems, and diverse environments, especially in laser with varying line-width, randomly varying atmospheric channels and dynamic alignment links. The line-width variation causes the phase of the optical signal to rotate [7]. The laser links are sensitive to the randomly inhomogeneous atmosphere and become unstable. The changing atmosphere leads to wave-front distortion and scintillation [8], [9]. The varying misalignment in the line-of-sight optical beam between the transmitter and receiver called pointing errors and also brings amplitude fluctuations [10], [11].These effects make the noise of the received signals constantly changing, which brings challenges to phase synchronization, makes the phase synchronization designed according to prior knowledge unreliable, will cause greater deviation, and even cause out-of-step.

Viterbi-Viterbi (VV) algorithm and its variants and blind phase search (BPS) algorithm are traditional phase estimating method [12], [13]. The accurate of the former is strongly dependent on the length of employed symbols [14]. The latter restores the symbol phase with a finite set of phases, and then compares their distances to the constellation points, the closest as a result [15]. We find that the traditional method adopts either fixed length or finite set, which is equivalent to using fixed bandwidth or limited variable bandwidth to deal with noise. Such approaches create a trade-off between steady-state accuracy and tracking speed.

We also find another limitation that the previous methods only consider the effect of phase noise, but do not fully consider the effect of amplitude noise. In fact, the magnitude of the amplitude has an impact on the performance. The scintillation in atmospheric channel will bring amplitude noise, and the smaller the amplitude is, the easier it is close to the decision threshold under phase noise, which will increase the probability of error.

Manuscript received 2 September 2023; revised 13 October 2023; accepted 25 October 2023. Date of publication 30 October 2023; date of current version 13 November 2023. *(Corresponding author: ShuPeng Zhang.)*

The authors are with the National Key Laboratory of Tunable Laser Technology, Harbin Institute of Technology, Harbin 150001, China (e-mail: zhangshupenghit@163.com; tanly@hit.edu.cn; majing@hit.edu.cn).

Digital Object Identifier 10.1109/JPHOT.2023.3328423

A combination of Viterbi-Viterbi phase estimation and linear kalman filter (LKF) was presented to improve estimating accuracy in low signal-to-noise case [16]. However, this combination algorithm used linear approximation could discard the nonlinear components and did not take the amplitude noise into account.

A third limitation is that atmospheric channels are time-varying, which makes it difficult for some methods originally using constant statistics. In particular, the scintillation caused by atmospheric turbulence makes the signal amplitude no longer constant. An improved adaptive square-root unscented kalman filter (ASRUKF) was proposed to compensation phase noise [17], in addition, it used the block amplitude mean value to normalize the receiving signal to ease the atmospheric turbulence problem. Precisely reducing amplitude noise could produce a more precise result.

In a time-varying environment, the model constructed by prior knowledge does not match the actual working state due to unexpected changes in dynamic system and statistical distribution. The inaccuracy of the system model and the statistical distribution of noise results in the deviation from the optimal estimation and even the non-convergence. To obtain the optimal phase noise estimation by kalman filter requires comprehensive and accurate prior knowledge of the optical coherent system and atmosphere channel, which cannot be done in practice. Considering the random fluctuations of channel state, a problem that needs to be addressed for kalman filter based algorithm that how to make assumptions about the process noise covariance and the measurement noise covariance consistent with their theoretical covariance at any time. This is an area that needs improvement of using kalman filter based algorithm to achieve phase synchronization. Embedding on-line estimation of noise statistics, the measurement noise and system noise parameters of kalman filter are corrected is a way to make the kalman filter consistent with the actual operating state. There are four classes on-line estimation of Gaussian process covariance estimation methods [18].They are maximum likelihood estimation, correlation method estimation, Bayesian estimation, covariance matching method. Covariance matching is one of the most common methods, and its basic idea is to make estimated innovation covariance consistent with their theoretical covariance [19]. An innovation based process noise variance estimation and a residual based measurement noise variance estimation use covariance matching method to make assumed variances consistent with their theoretical covariance [17]. In the literature reviewed so far, almost all of them use covariance matching method in phase synchronization. The basic idea of correlation methods is to correlate innovations. A set of equations is derived relating the systems parameters to the observed autocorrelation function and these equations are solved simultaneously for the unknown parameters [20]. Both the maximum likelihood method and the Bayesian method can give relatively accurate estimates, but the calculation amount of the two methods is large, and they are based on the assumption that the dynamic deviation is time invariant, and do not match the operating conditions [21].

Wireless coherent optical communication systems need accurate phase synchronization to meet the coherent conditions, recover information correctly from the carrier, and maximize the advantages of coherent communication. In the past, phase synchronization methods only consider phase noise, but in atmospheric channel, scintillation makes amplitude noise more serious, so the consideration of amplitude noise becomes particularly important. Due to the scintillation, low SNR will occur. The pre-decision needs to be based on certain performance, otherwise the pre-decision will cause a large number of false symbol decisions, resulting in inaccurate estimation and filter divergence, so the modified extended kalman filter (MEKF) cannot be directly applied in atmospheric channels. As the atmospheric channel is time-varying, the performance of the constant value statistics method in the time-varying channel will become unreliable, so the fractionally-spaced blind equalization also cannot be used directly. Additionally, the noise of atmospheric channel is time-varying, so is the compound of all kinds of noise. The kalman filter designed with prior knowledge may not be consistent with the actual working state. Setting low constant parameter will cause the estimate to deviate from the optimal estimate, and setting high parameter will cause the filter to diverge.

In this paper, a combination of fractionally-spaced dual-mode modified constant modulus algorithm (MCMA) and directed decision (DD) blind equalization (FSE-MCMA+DD) and adaptive kalman filter (AKF) is proposed. The FSE-MCMA+DD equalization preliminarily was used to reduce amplitude and phase noise with updating its weight coefficients adaptively with the receiving signals changing according to the real-time situation. The output was prepared to optimize the following pre-decision which part they shared used in sequential modified extended kalman filter (MEKF) which more thoroughly eliminated amplitude and phase noise. FSE-MCMA+DD equalization improves the performance of pre-decision, enabling MEKF to work directly in atmospheric channel at low signal-to-noise ratio. At the same time, more accurate feedback of MEKF can more thoroughly reduce the influence brought by time-varying channel. This makes the steady state error of FSE-MCMA+DD lower, the convergence faster, and the FSE-MCMA+DD can be directly used in the atmospheric channel according to the original design. The combination constitutes a virtuous circle. And then we will respectively use covariance matching (CM) method and Autoregressive (AR) method to estimate the variance of the noise, especially AR method, has not been seen in literature for phase synchronization in wireless optical communication. The estimated result is used to update the noise parameter of AKF that makes the parameter of the AKF match the actual noise state. The AKF will be better to adapt to the time-varying noise brought by the atmospheric channel and optical communication system, so that the adaptive kalman filter is more accurate and the system with adaptive parameter scheme has larger and wider line width selection compared with the constant parameter design, and is more suitable for the dynamic channel conditions.

The remained of this paper is organized as follows. In Section II, the system model, channel statistics are introduced. In Section III, a combination of FSE-MCMA+DD and AKF implementing is proposed and its principle of operation is described. In Section IV, the simulation results are discussed. Finally, conclusions are provided in Section V.

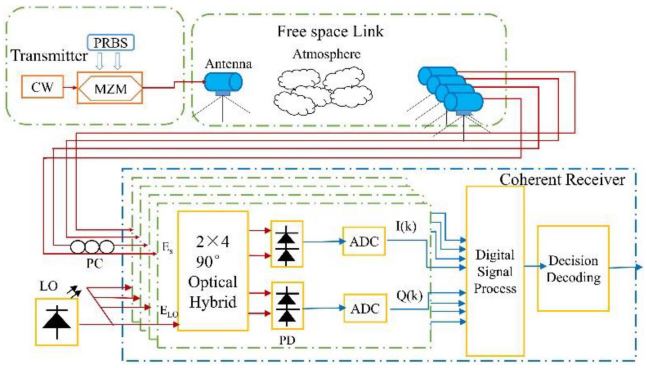

Fig. 1. Schematic of free space coherent optical communication system.

II. System Constitution and Channel Statistics

Four receiving apertures wireless optical coherent communication system with Pi/4-QPSK modulation is considered in this paper. The QPSK modulated signal is radiated via a single aperture transmitter, propagating through the atmospheric channel and received by four receiving apertures to be coherent with the same local oscillator. Schematic diagram of system is shown in Fig. 1.

The transmitted QPSK signal can be expressed as

$$E_{TX}(t) = \sqrt{P_T}\exp\left(j\left(2\pi\nu_c t + \Phi(t) + \phi_{lw}(t)\right)\right) + n(t) \tag{1}$$

Where transmitted optical power P_T, carrier frequency ν_c, and modulated phase $\Phi(t)$, and additive white Gaussian noise (AWGN) $n(t)$. The phase noise $\phi_{lw}(t)$ is caused by the line-width of laser and can be modeled by two random walk processes with a step size that varies according to a normal distribution [22].

The signals propagating through atmospheric channel are received by four apertures which are mutually uncorrelated, one of which at lth aperture can be described as

$$I_l = 2R\sqrt{\xi_l}E_{TX}(t) + n_l \tag{2}$$

Where $\xi_l = \xi_{att} \bullet \xi_{sci}$ is intensity fluctuation, ξ_{att} is the constant loss due to divergence and ξ_{sci} is the random irradiance fluctuation caused by atmospheric turbulence scintillation and $n_l(t)$ is the AWGN. The most common statistical model for the atmospheric turbulence scintillation is log-normal distribution [23]. That means that the distribution of logarithm of intensity fluctuation is Gaussian distribution. Rytov variance, $\sigma^2_{Rytov}$is used to describe scintillation when using the Kolmogorov spectrum and is also used to divide the atmospheric turbulence conditions, such as $\sigma^2_{Rytov} < 1$ for weak turbulence.

$$\sigma^2_{Rytov} = 1.23C_n^2k^{7/6}L^{11/6} \tag{3}$$

Where C_n^2 is atmospheric structure constant which also is a measure for scintillation strength. In this paper, we choose 0.05, 0.25, 0.55 as the values of Rytov variance, and the corresponding value of C_n^2 are $2.51\times10^{-15}m^{-2/3}$, $1.25\times10^{-14}m^{-2/3}$, $2.76\times10^{-14}m^{-2/3}$. $L$is the distance, $k = 2\pi/\lambda$ is wave number.

The received signal is mixed with local oscillator (LO) laser in 90° optical hybrid. The output signals are converted to electrical signals by two balanced photodetectors (BPDs), and the in-phase (I) and quadrature (Q) baseband signal outputs can be expressed as

$$r_I(t) = 4R\sqrt{P_s(t)P_{Lo}}\cos\left(2\pi\Delta\nu t + \Phi(t) + \phi_n(t)\right) + n_I(t) \tag{4}$$

$$r_Q(t) = 4R\sqrt{P_s(t)P_{Lo}}\sin\left(2\pi\Delta\nu t + \Phi(t) + \phi_n(t)\right) + n_Q(t) \tag{5}$$

Where P_{Lo} is the output average power of LO laser, R is the detector responsivity, $\Delta\nu$ is the difference between the carrier frequency and LO laser frequency, $\phi_n(t)$ is the phase noise including the term $\phi_{lw}(t)$ caused by the line-width of the transmitted and local lasers $\Delta\nu_c$ and phase noise term $\phi_{wd}(t)$ caused by atmosphere turbulence. The phase fluctuation ϕ_{wd} caused by the atmospheric turbulence can be modeled by zero mean normal distribution [24]. In order to study phase distortion caused by atmosphere, the classic statistics of phase variance σ^2_φ is extended to consider model compensation. In the model compensation, Zernike polynomials is used to denote residual phase variance [25]. It is well known that the residual phase variance after model compensation of J Zernike polynomial terms is described as

$$\sigma^2_\varphi = C_J(D/r_0)^{5/3} \tag{6}$$

Where C_J is about the order of the correction of phase distortion by adaptive optical system. When no terms are corrected by active model compensation, the coefficient $C_J = 1.0299$. D is the diameter of receiver aperture, and r_0 is Fried parameter. For plane waves and Kolmogorov turbulence, $r_0 = \left(0.423k^2C_n^2L\right)^{-3/5}$ [26].

From above, the homodyne detecting received signal can represent as

$$\begin{aligned} r(t) &= r_I(t) + jr_Q(t) \\ &= 2R\sqrt{P_s(t)P_{Lo}}\exp\left(j\left(2\pi\Delta f t + \phi_n(t)\right)\right) + n(t) \end{aligned} \tag{7}$$

In the ideal situation, the deviation of the transmitter and receiver is set zero, $\Delta f = 0$. The noise term $n(t)$ is divided into the In-phase component $\tilde{n}$ and the Quadrature component $\bar{n}$. The received power can represent as

$$P_s(t) = \xi_l P_t \tag{8}$$

And the amplitude h can be expressed as

$$h = 2R\sqrt{\xi_l}\sqrt{P_tP_{Lo}} \tag{9}$$

$$\begin{aligned} r(t) &= 2R\sqrt{\xi_l}\sqrt{P_tP_{Lo}}\exp\left(j\phi_n(t)\right) + n(t) \\ &= \left(h(t) + \tilde{n}(t)\right)\exp\left(j\left(\phi_n(t) + \bar{n}(t)\right)\right) \end{aligned} \tag{10}$$

From the above equation, the amplitude noise and the phase noise combine as hybrid noise, which pollutes the received signal, and at the meanwhile we can consider amplitude noise as multiplicative noise. From the constellation, we will observe that $(\cos(\Phi(t)), \sin(\Phi(t)))$ changes to $((h+\tilde{n})\cos(\Phi(t)+\phi_n(t)+\bar{n}), (h+\tilde{n})\sin(\Phi(t)+\phi_n(t)+\bar{n}))$ because of the hybrid noise.

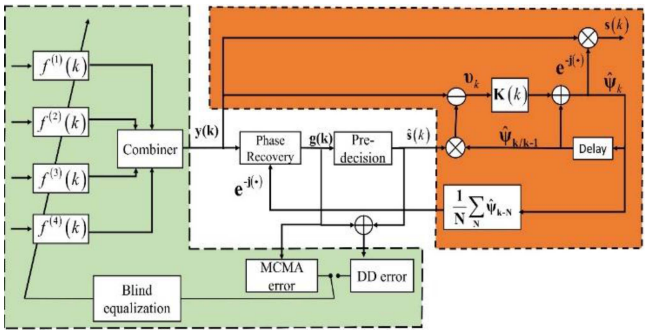

Fig. 2. Combination of FSE-MCMA+DD and MEKF.

If the signal is only polluted by amplitude noise, its coordinate can be expressed as $(h\cos(\Phi(t)), h\sin(\Phi(t)))$, and the multiplicative noise does not interface the decision of symbol. But the shorter the radius is, the closer it is to the decision threshold. The presence of additive noise will increase the probability of decision mistakes, and that will magnify the symbol error ratio. Therefore, we can reduce the hybrid noise, especially the amplitude noise, to improve the accuracy of decision and degrade symbol error ratio (SER).

Through analog-to-digital conversion of I and Q photocurrents of each branch, baseband digital signals are obtained. Frequency deviation and delay are eliminated through frequency recovery and timing synchronization. Then the baseband signals will be send into FSE-MCMA+DD equalization, and then AKF. After these, the outputs are sent for symbol decision to get the final performance.

III. Principle of Operation

A combination of FSE-MCMA+DD and MEKF is introduced in Fig. 2.

The part of the "L" type green background is the spatial diversity fractionally-spaced blind equalizer, while the part of the "7" type red background is the modified extended Kalman filter, and the part without background in the middle is the part shared by them.

The FSE-MCMA+DD equalization preliminarily was used to reduce amplitude and phase noise with updating its weight coefficients adaptively with the receiving signals changing according to the real-time situation. The output was prepared to optimize the following pre-decision which part they shared used in sequential modified extended kalman filter which more thoroughly eliminated hybrid noise.

In atmospheric channel, the existence of multiplicative amplitude noise which aggravates the instability of channel will lead to the emergence of low signal-to-noise ratio (SNR), and the modified extended kalman filter needs to use pre-decision, while low SNR will cause the pre-decision to be unreliable, resulting in impossible to estimate exactly and even filter divergence. Therefore, the modified extended kalman filter cannot be directly applied in atmospheric channel. At the same time, the phase noise caused by wave-front distortion and laser line-width is also time-varying, so the processing method using constant statistics is also limited. As a result, fractionally-spaced blind equalization also cannot be directly applied in atmospheric channel. But combining them together can change these unable to use and achieve better performance.

FSE-MCMA+DD equalization is used to eliminate symbol and channel interference to the signal. It can be divided into two parts, the first part is the reception of fractionally-spaced signal, and the second part is the realization of equalization algorithm to adjust the taps. The equalization of symbol rate can only eliminate the inter-symbol interference due to the close proximity of the spectrum, while the frequency spectrum of fractionally-spaced equalization has the channel information, so the influence of the channel on the signal can be reduced [27]. Since the change of atmospheric turbulence is slow relative to the signal rate, the signal is correlated in time. Therefore, using four apertures spatial diversity to receive instead of time diversity is equivalent to oversampling, and the reception of uncorrelated fractionally-spaced signal is input of equalization. Spatial diversity can be combined in a natural way by fractionally-spaced equalization. Then MCMA and DD dual-mode equalization algorithm is used to adjust the taps according to the error between the output of equalization and the expectation or desired signal. Actually it is not accurate to directly use the expectation and the desired signal in time-varying situation, because they are always changing in atmosphere channel. A solution to ease the effect of time-varying channel by using input signals dividing their modulus in the cost function [28], it also adds much complexity when calculate the derivative. The combination approach to address the effect of time-varying channel will be explained later.

In order to estimate hybrid noise to compensate the received signal $r_k$and recover the transmitted signal s_k, extended kalman filter is used. Lowercase k represents time instant. Unlike traditional phase estimation algorithm, only partial phase distortion and additive noise damage are recovered and unlike amplitude attenuation in fiber [29], there are not only phase distortion θ_k, but also multiplicative noise related to signal amplitude $|s_k|e^{\log h_k}$in atmosphere channel, h_k representing the scintillation in amplitude. In order to compensate the amplitude and phase noise damage as far as possible, the phase estimate is changed from the original real value φ_k to the complex valueψ_k. Complex phase ψ_k can include phase noise and amplitude noise resulted from atmosphere turbulence and the optical system, such as the noise caused by the line-width effects and shot noise. The design of MEKF is based on extended kalman filter with state variable changed from the original real value φ_k to the complex valueψ_k. The extended kalman filter is obtained by using kalman filter to linearize the nonlinear part through Taylor series expansion. Kalman filter can provide a general framework for the optimal estimation of signal phase deviation, which evolve according to a given dynamical system model. Therefore, the extended kalman filter can adaptively use an optimal bandwidth to balance the steady-state accuracy and tracking capability so that the mean square error between the estimated signal phase error and the actual phase error of the received signal is minimized. The state variable turns to complex phase, the real part represents phase noise, the imaginary part represents amplitude noise, and the phase and amplitude noise

are considered at the same time. Through iterative process, the optimal estimate of the complex phase is output, which is then used to reduce the amplitude and phase noise more completely in wireless channel.

In the middle, FSE-MCMA+DD and MEKF share a pre-decision part. The pre-decision is used to adjust the DD taps and as measurement coefficient in MEKF measurement equation. More accurate pre-decision will make FSE-MCMA+DD have accurate steady state error and improve tracking capability and also will enables MEKF to obtain more accurate complex phase measurement and keep uncertainty of measurement of MEKF in proper level. But MCMA only has limited phase recovery capability, while DD is sensitive to phase noise, and it is mentioned before that in atmospheric channel, direct application of MCMA and DD is inaccurate. To solve this problem, the average of latest complex phase estimates of a certain length from MEKF is used to restore the output of the equalizer to mitigate the effect of atmospheric channel, because these complex phase are output of MEKF tracking the changing channel. This behavior not only improves the phase recovery ability of the equalizer, but also enables the equalizer to use the expectation or expected signals to calculate the error as originally designed.

In the real situation, the noise parameters of system noise and measurement noise set by prior knowledge may not match the actual working state. Especially when the signal-to-noise ratio span is large and there is effect of atmospheric turbulence at the same time, it is difficult to include so many states with the same parameter to make each state have better performance. Often taking into account the low signal-to-noise ratio, then the condition of the high signal-to-noise ratio is no longer corresponding to the working range of the same parameter setting, and there is a performance deviation. Another situation is that the line-widths of transmitter laser and local oscillator laser become larger. Larger line-widths require greater tracking capability. Constant parameter limits steady-state error and tracking ability. In order to solve this problem, we use the innovation series that is deviation between measurement and prediction to fit AR model, and estimate the noise variance by this model. Then the variance is used to update measurement equation noise parameter of MEKF. It allows MEKF to adapt to the working state at any time. It is worth mentioning that this noise is a virtual noise concept, because it includes the bias caused by inaccurate system models and noise distribution and real noise variation.

The above process will be described by the following flow:

The baseband signals after frequency recovery and timing synchronization at each branch will be send into FSE-MCMA+DD equalization. The source symbol sequence $\{S_k\}$ with period T is transmitted through atmosphere channel with impulse response $\boldsymbol{h}$. $\boldsymbol{r}$ is the received baseband signal interfered by additive noise $\boldsymbol{w}$, which can be expressed as

$$\boldsymbol{r}_k = \sum_{i=0}^{L_h} \boldsymbol{h}_i s_{k-i} + \boldsymbol{w}_k \tag{11}$$

The impulse response of the sub-channel l ($l = \{1, 2, 3, 4\}$) is obtained from the channel vector $\boldsymbol{h}$, where $L_h + 1$ is the length of the impulse response of the sub-channel.

The output of fractionally-spaced blind equalization can be described as

$$y_k = \sum_{i=0}^{L_f} \boldsymbol{f}_i^H \boldsymbol{r}_{k-i} = \boldsymbol{f}^H \boldsymbol{r}_k \tag{12}$$

Where $\boldsymbol{f}_i$ representing the baud rate the column vector composed of the i th tap of each sub-equalizer,$i = 0, 1, 2, \ldots, L_f$ and the length of the tap coefficient vector of the fractionally-spaced blind equalizer is $l \times (L_f + 1)$, in this paper$L_f = 6$. H denotes conjugate transpose.

Then, the signal is input into the dual mode blind equalizer which is core principle to control the tap $\boldsymbol{f}$. In order to alleviating the influence of time-vary channel and improving phase compensation ability, phase recovery is added. $\hat{\phi}_k$ is the average value of the past estimates of a certain length that is fed back by subsequent MEKF, in this paper, N = 10. g_k is the output after phase recovery.

$$\hat{\phi}_k = \frac{1}{N} \sum_{N} \hat{\psi}_{k-N} \tag{13}$$

$$g_k = y_k \cdot \exp\left(-j\hat{\phi}_k\right) \tag{14}$$

MCMA or DD is used to achieve equalization. Their taps updating equations because of adding phase recovery will be express as

$$f_{k+1} = f_k - \mu_{MCMA} \cdot error^*_{MCMA} \cdot y_k \cdot \exp\left(-j\hat{\phi}_k\right) \tag{15}$$

Where μ_{MCMA} is the update step-size parameter and is set to 10^{-3}, $error^*_{MCMA}$ is the conjugate of the error of MCMA.

$$f_{k+1} = f_k - \mu_{DD} \cdot error^*_{DD} \cdot y_k \cdot \exp\left(-j\hat{\phi}_k\right) \tag{16}$$

Where μ_{DD} is the update step-size parameter and is set to 10^{-3}.

The received eye pattern is usually of low quality at the beginning, in this case the algorithm may not converge due to the high probability of wrong decision. Therefore, MCMA blind equalization algorithm based on the statistical characteristics of symbols is first adopted, but MCMA has a large steady-state error [30]. In order to overcome this shortcoming, the directed decision (DD) algorithm based on the instantaneous characteristics of symbols is used to reduce the steady-state error of MCMA. The switching between the two blind equalization algorithms is through a decision circle. The MCMA algorithm is used to update the tap coefficient when the mean square error (MSE) is outside the decision circle, and when the mean square error is inside the decision circle, the DD algorithm is used to update the tap coefficient (17) shown at the bottom of the next page.

Where $d = 0.4$ is the decision threshold for switching and $0 < d < (L/2)^2$ is satisfied, where L is the minimum distance between QPSK constellation points.

An MSE estimator with forgetting factor is introduced to estimate the MSE in the iterative process in real time:

$$MSE_k = \lambda \cdot MSE_{k-1} + (1 - \lambda) \left| g_k - \hat{s}_k \right|^2 \tag{18}$$

Where the forgetting factor λ is 0.99.

After equalization, the following MEKF is used to phase recovery. The output of blind equalization y_k is the input of MEKF. The system equation and measurement equation of modified extended Kalman filter:

$$\psi_k = \psi_{k-1} + w_k \tag{19}$$

$$r_k = \hat{s}_k e^{j\psi_k} + v_k \tag{20}$$

Where ψ_k is the complex phase, the real part represents phase noise, the imaginary part represents amplitude noise, and the phase and amplitude noise are considered at the same time. r_k is the received signal. $\hat{s}_k$ is the pre-decision of original symbol s_k. w_k and v_k are assumed zero mean Gaussian noise and their variances are Q_k, R_k. Under Gaussian noise assumption, MEKF performs optimal filtering [31]. In this paper, the variances of noise w_k and v_k are set to be 10^{-2} and 10^{-1} in MEKF respectively.

In order to make the kalman filter consistent with the actual operating state, we use CM and AR methods to update measurement noise parameter respectively. The innovation υ_k of kalman filter is the difference between measured and predicted values.

$$\upsilon_k = r_k - \hat{s}_k e^{j\psi_{k/k-1}} \tag{21}$$

Where $\psi_{k/k-1}$ is the predicted complex phase noise. r_k is the measurement value. $\hat{s}_k$ is the pre-decision of the transmitter symbol that is not known. Using the real measurement symbol minus the transmitter symbol we determined by certain rules with predicted amplitude and phase noise, we can obtain the innovation $\upsilon_k$about fresh information and calculate its covariance in CM methods.

$$\hat{C}_\upsilon = \frac{1}{m}\sum_{i=0}^{m-1} \upsilon_{k-i}\upsilon_{k-i}^H \tag{22}$$

The statistical average of the square of the innovation covariance matrix can be viewed as statistical smoothing through a window of length m.

Through the following relationship, we will get the estimated variance of measurement noise$\hat{R}_k$. Use $\hat{R}_k$ to update the variance of measurement equation noisev_k.

$$\begin{aligned}\hat{R}_k &= \hat{C}_\upsilon - H_k \hat{P}_{k/k-1} H_k^H \\ &= \hat{C}_\upsilon - H_k \left(F_{k-1}P_{k-1}F_{k-1}^H + Q_{k-1}\right) H_k^H\end{aligned} \tag{23}$$

Or we can use another way. After MEKF has been running for some time, in AR methods, an innovation based time series with length M can be obtained $\upsilon_k, \upsilon_{k-1}, \cdots, \upsilon_{k-(M-1)}$. Firstly, the autocorrelation function is calculated.

$$R_\upsilon(m) = \frac{1}{M}\sum_{n=0}^{M-1-|m|} \upsilon(n)\,\upsilon(n+m), |m| \le M-1 \tag{24}$$

The general AR (1) model for a discrete innovation sequence υ_k is specified by the recursion.

$$\upsilon_k = \alpha_{1,1}\upsilon_{k-1} + \eta_k \tag{25}$$

Where η_k is a white Gaussian noise sequence with variance σ_η^2. And the coefficient $\alpha_{1,1}$ and the variance σ_η^2 can be obtained through the Yule-Walker equations using the autocorrelation function $R_\upsilon(m)$ [32]. Final prediction error criterion function value FPE (1) also can be calculated.

Final prediction error (FPE) criterion function is used to decide the order of the AR model.

$$FPE(P) = \sigma_P^2 \frac{M+(P+1)}{M-(P+1)} \tag{26}$$

The order P corresponding to the minimum value will be the order of the model. σ_P^2 is the estimate of the prediction error power of the P-order AR model. M is the number of data.

Then, according to the Levinson-Durbin (L-D) algorithm, the iterative operation is carried out and the coefficients and variances of every order of AR model is obtained until the final prediction error criterion function reaches the minimum value, and the order P is determined. Then the $AR(P)$ model can be determined, and the variance of the noise $\hat{R}_k$ can be estimated to update the variance R_k of measurement noise v_k. The MEKF is upgraded to AKF. The optimal estimation complex phase from AKF will be used to recover the transmitted symbol more accurately.

$$s_k = r_k e^{-j\hat{\psi}_k} \tag{27}$$

IV. Simulation Results

In this section, Pi/4-QPSK based FSO system is considered. The system and channel models adopted in the simulations were shown in Section II. The distance between each receiver aperture is assumed greater than the coherent length of atmosphere, so each sub-channel is assumed affected by i.i.d. Log-Normal atmospheric turbulence. 20 sweep iterations were done for the same signal-to-noise ratio to ensure that a relative accurate SER can be obtained; for each iteration, 2^{14} symbols pseudo random symbol sequence are generated for SER test, and a constant channel fading is considered over the duration of a frame of symbols (Coherent time), changing to a new independent value from one frame to the next. First of all, the application scope of each scheme will be found according to the selection of line-width, and the performance will be compared under which line-width according to the conclusion. Then, the performance of each scheme will be compared under the presence or absence of atmospheric conditions. Other parameters presented in the simulations are summarized in Table I.

$$J_k = \begin{cases} E\left[\left(real(g_k)^2 - \gamma_R\right)^2 + \left(imag(g_k)^2 - \gamma_I\right)^2\right] & MSE > d \\ E\left[\left(g_k^2 - \hat{s}_k^2\right)^2\right] & MSE <= d \end{cases} \tag{17}$$

TABLE I
PARAMETERS FOR SIMULATION

Parameter	Value	Parameter	Value
Wavelength	1550nm	Symbol Rate	1G Baud
Line-width	2-15kHz	Coherent time	$1\times10^{-6}s$
Constant loss	3dB	Rytov variance	0.05,0.25,0.55
Aperture diameter	5cm	Wave-front distortion variance	0.07,0.13,0.2
Distance	1000m		

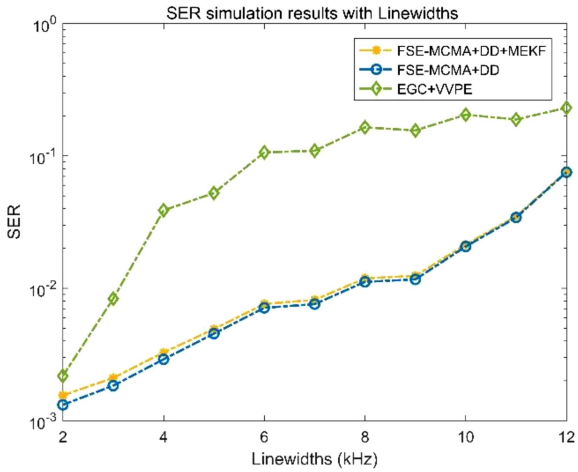

Fig. 3. SER performance versus Line-widths 2kHz-12kHz.

Four schemes, Equal Gain Combining followed by Viterbi-Viterbi Phase Estimation, FSE-MCMA+DD, FSE-MCMA+DD-MEKF and FSE-MCMA+DD-IEKF, are firstly considered. For single input multiple outputs (SIMO), EGC is the most commonly used combining technique because equal gain combining is close to Maximal Ratio Combining (MRC) in performance and it is simple in implementation [33]. Through coherent receiving of multiple signals and the light of local oscillator laser, the performance close to MRC performance can be obtained by EGC in the electrical domain, and then can be further improved by the following VVPE. VVPE is also most commonly used phase compensation technology. The other three schemes are FSE-MCMA+DD, FSE-MCMA+DD-MEKF, and FSE-MCMA+DD-IEKF. The difference of the former two schemes is that compensating phase is the mean of latest estimates of a certain length or the optimal estimate from MEKF. The difference of the latter two schemes is that using pre-decision or the transmit symbol as measurement coefficient. Secondly, the combination of FSE-MCMA+DD-AKF improved by CM or AR method is respectively compared with FSE-MCMA+DD-MEKF in different conditions.

At first, we examine the options based on the line-width factor. This will make the limitations of constant parameter schemes clearer.

In Fig. 3, The SER performance of FSE-MCMA+DD-MEKF compared with that of Equal Gain Combining (EGC) and Viterbi-Viterbi phase estimation (VVPE) as the line-width of the laser changes from 2kHz to12kHz. EGC+VVPE is added as a comparative item in order to illustrate that FSE-MCMA+DD-MEKF with constant parameter also has certain steady-state error accuracy and tracking ability. With SER $= 10^{-2}$ as the boundary, EGC+VVPE almost exceeds the boundary at 3kHz, while FSE-MCMA+DD-MEKF will not exceed until 8kHz, which indicates that FSE-MCMA+DD-MEKF has better tracking and phase compensation capabilities. If more than 3kHz, there is almost no comparison between the two, so in order to observe the performance comparison between the two, 3kHz is selected as the line- width for research firstly.

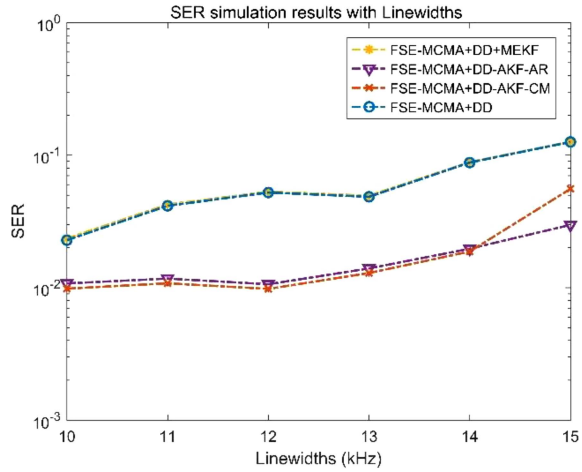

Fig. 4. SER performance versus Line-widths 10kHz-15kHz.

Despite MEKF has better performance, constant parameter limits its application, for example, it can only be used when the line-width is less than 8 kHz. In Fig. 4, the selection range of line-width is extended to 15 kHz, and the performances of the scheme with noise parameter corrected and the constant parameter scheme are compared. It can be seen from the figure that the performances of the adaptive scheme AKF-CM and AKF-AR are better than that of the fixed parameter setting MEKF. Still using SER $= 10^{-2}$ as the performance boundary, MEKF can only work to 8kHz, but AKF can be extended to 12kHz, which shows that through adaptive adjustment of parameters, the original working range can be extended to meet the harsher working conditions. Therefore, in order to better compare the performance of AKF and MEKF, the line-width will be then expanded to 12kHz.

In Fig. 5, in comparison, without atmospheric turbulence, only line-width effects and constant attenuation are considered. The figure shows the condition of each scheme at 3kHz line-width. It can be seen from the SER analysis that compared with the performance of single-channel reception, the performance of multi-channel reception can be improved by the combining in the electrical domain after coherent with the local oscillator.

From the above SER, it can be found that the performance trend of FSE-MCMA+DD and FSE-MCMA+DD-MEKF is consistent with that of EGC+VVPE. All decreased with the increase of SNR. For the same SER, the performance of FSE-MCMA+DD-MEKF is nearly 2dB better than that of EGC+VVPE, and the performance of FSE-MCMA+DD-IEKF is 3-4dB better than that of EGC+VVPE.

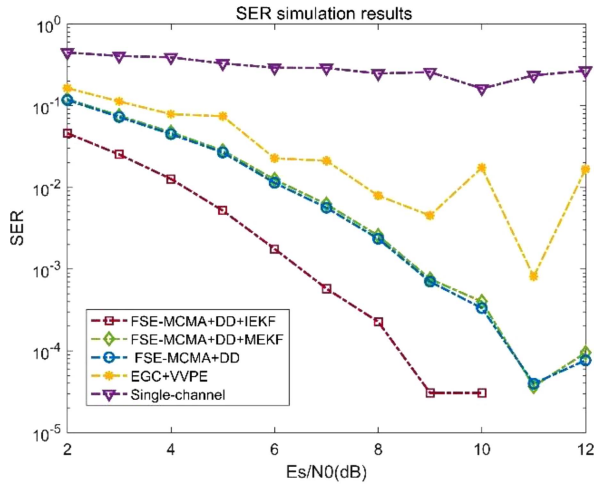

Fig. 5. SER performance at 3kHz.

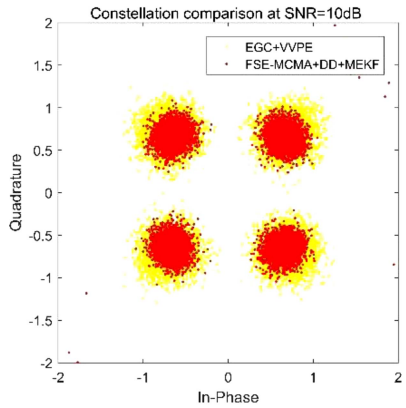

Fig. 6. Constellations at SNR = 10 dB.

In Fig. 6, the constellation with SNR of 10dB, the constellation points of each symbol are clearly separated, and the amplitude and phase noise reduction of FSE-MCMA+DD-MEKF is more thorough than that of EGC+VVPE, so it is easy to find that the signal quality of FSE-MCMA+DD-MEKF is better. To better illustrate the performance of the combined scheme, the changes in performance can be seen more clearly through MSE.

In Fig. 7, firstly, the overall performance can be ranked, from high to low performance, FSE-MCMA+DD-IEKF>FSE-MCMA+DD-MEKF>EGC+VVPE>FSE-MCMA+DD. Secondly, after stabilization, the MSE of FSE-MCMA+DD-MEKF is 1-2dB lower than that of EGC+VVPE at the same SNR. Thirdly, by comparing MSE, it can be found that the performance of FSE-MCMA+DD-MEKF is improved compared with that of FSE-MCMA+DD, and FSE-MCMA+DD-MEKF is reduced to the same MSE performance level faster, which indicates that FSE-MCMA+DD and MEKF combination optimizes the steady-state accuracy and the speed of convergence of FSE-MCMA+DD.

In Fig. 8 and 9, different Rytov variances and wave-front distortion phase variances are selected to investigate the performance changes of several schemes under different turbulence conditions.

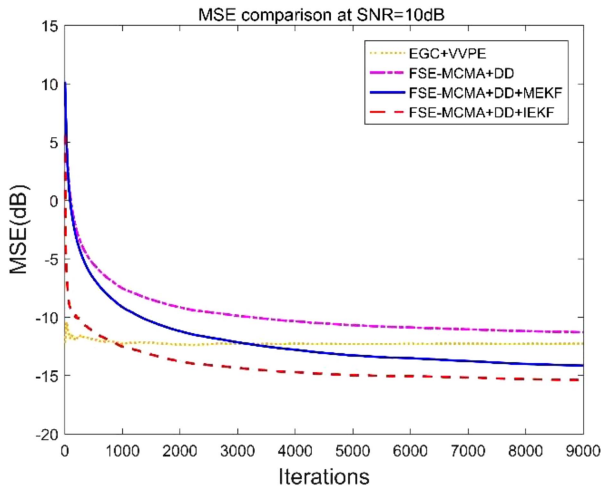

Fig. 7. MSE at SNR = 10dB.

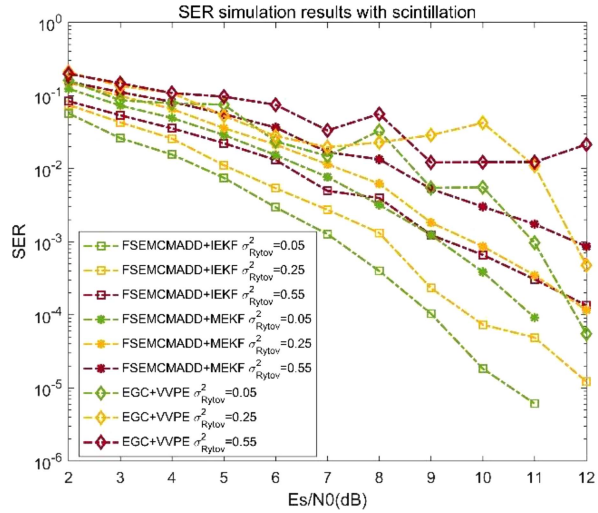

Fig. 8. SER simulation results with Rytov variances.

Fig. 8 illustrates the performance of the system under three different Rytov variances. The performance hierarchy is FSE-MCMA + DD-IEKF > FSE-MCMA + DD-MEKF > EGC + VVPE, where IEKF has a 2dB improvement over MEKF in the same SER, and MEKF has a 1-2dB over EGC+VVPE.

Fig. 9 shows the performance of the system under three phase variance conditions of different wave-front distortions. It can be found that the trend of several schemes is similar to that without turbulence, and SER will decrease with the increase of SNR. However, when the phase variance of wave-front distortion increases, the performance will get worse. As the phase variance of wave-front distortion changes from small to large, it can be seen that the performance area of SER shifts upward. It can be found that EGC+VVPE only has SER lower than 10^{-2} under the condition of the lowest wave-front distortion phase variance and high SNR, while MEKF can obtain a performance lower than SER = 10^{-2} under the condition of medium wave-front distortion variance and high SNR, and the performance is getting better and better with the increase of SNR. Only IEKF can achieve this at high wave-front distortion variance.

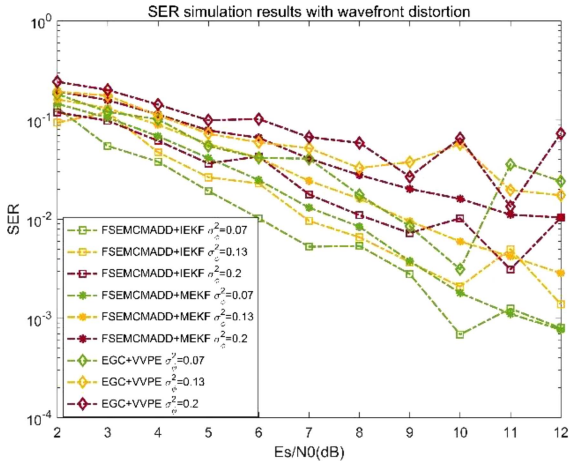

Fig. 9. SER simulation results with wave-front distortion phase variances.

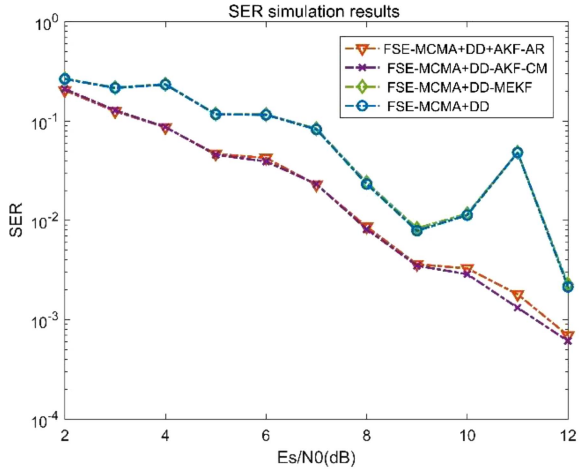

Fig. 11. SER simulation results at line-width 12kHz.

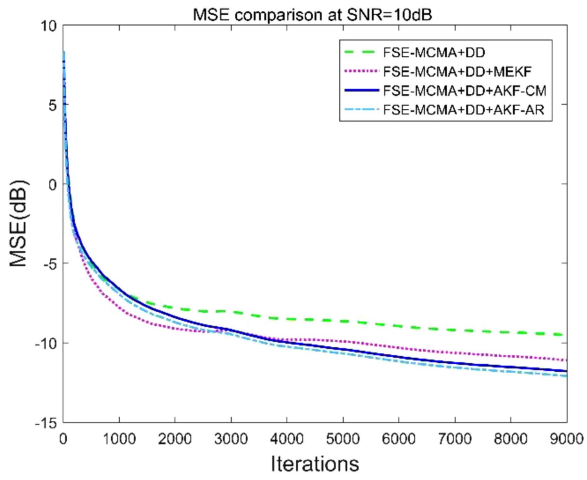

Fig. 10. MSE at SNR = 10dB.

Through the above simulation, it can be seen that the proposed FSE-MCMA+DD-MEKF scheme improves the MSE by 1-2dB compared with EGC+VVPE, and has higher tracking capability and can handle a lager range of line-width. In addition, the comparison of constellation also shows that the combination can improve the signal quality. The effect of amplitude noise and phase noise reduction is achieved, and MEKF is also 1-2dB better than EGC+VVPE at SER.

Then, according to the conclusion of line-width before, in order to better compare the performance of AKF and MEKF, the line-width will be then expanded to 12kHz. MEKF was improved respectively by means of covariance matching method and autoregressive method, and two AKF schemes, FSE-MCMA+DD-AKF-CM and FSE-MCMA+DD-AKF-AR, were formed. The performance of FSE-MCMA+DD-MEKF and FSE-MCMA+DD-AKF are compared to explain the characteristics of AKF. The performance of FSE-MCMA+DD-AKF-CM and FSE-MCMA+DD-AKF-AR was compared at the same time to understand the characteristics of different adaptive methods.

In Fig. 10,with MSE we can see the performance changes more clearly and can sort the performance:FSE-MCMA+DD-AKF-AR>FSE-MCMA+DD-AKF-CM>FSE-MCMA+DD-MEKF>FSE-MCMA+DD.It can be seen that the performances of the combination schemes of AKF with using the updated noise variance estimation are improved compared with that of the original MEKF. In addition, AKF-AR performs slightly better than AKF-CM, because the CM method uses the average of the covariance to estimate the variance of the noise, which is equivalent to AR with only constant terms. AKF-AR uses L-D method to get the estimated variance of each order recursively, and then uses FPE to determine the optimal order, and takes the corresponding variance as the final output. Since the optimal order is not necessarily order zero, the performance of AKF-AR will be better than that of AKF-CM.

In Fig. 11, after expanding the line-width, the performance of each scheme of FSE-MCMA+DD-AKF is better than that of FSE-MCMA+DD-MEKF, and the SER performance of AKF is 1-2 dB better than that of MEKF. This shows that the adaptive algorithm can achieve better performance under more stringent conditions by adjusting the original fixed parameters, so that the system can adapt to larger working conditions.

In Figs. 12 and 13, different Rytov variances and wave-front distortion phase variances are selected to investigate the performance changes of several schemes under different turbulence conditions.

In Fig. 12, Rytov variance from low to high, all schemes show a trend of lower symbol to error ratio with the increase of SNR, and SER performance will gradually deteriorate with the gradual increase of Rytov variance. In general, the SER performance regions corresponding to small and large Rytov variance can be distinguished. The performance level of AKF scheme and MEKF scheme can be clearly distinguished, and AKF scheme is better than MEKF scheme. MEKF can only receive the performance below SER = 10^{-2} under the condition of the lowest Rytov variance and the maximum SNR, and the overall performance area is worse than SER = 10^{-2}, while the scheme of AKF, with the same Rytov variance, receives better and better performance than SER = 10^{-2} after the signal-to-noise

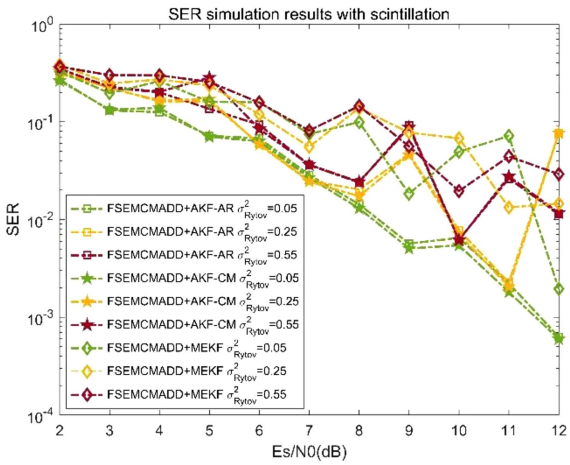

Fig. 12. SER simulation results with Rytov variances.

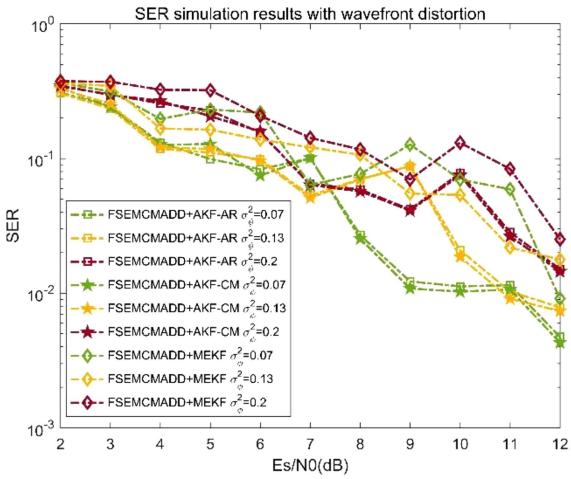

Fig. 13. SER simulation results with wave-front distortion phase variances.

ratio of 8dB. In other Rytov variances, AKF can also gain better performance than SER = 10^{-2} when the signal-to-noise ratio is high. In Fig. 13, it can be found that the trend of these schemes is similar to that of scintillation conditions, but the SER performance deteriorates with the increase of the phase variance of wave-front distortion. The performances of FSE-MCMA+DD-AKF-AR and FSE-MCMA+DD-AKF-CM are basically the same and better than FSE-MCMA+DD-MEKF. It can be observed that only when the phase variance of the wave-front distortion is low and medium, and the SNR is high, can the AKF schemes achieve performances lower than SER = 10^{-2}, and the following SER performances decrease with the increase of the SNR, which reflects that the influence of wave-front distortion on the receiving performance is relatively serious.

V. Conclusion

In this paper, we have a research of the phase synchronization of pi/4-QPSK modulated wireless optical coherent communication system in Log-Normal atmospheric turbulence channel. The phase synchronization performance of FSE-MCMA+DD-MEKF and EGC+VVPE schemes under 3kHz line-width and the phase synchronization performance of FSE-MCMA+DD-AKF and FSE-MCMA+DD-MEKF under 12kHz line-width are simulated respectively. At 3kHz line-width, FSE-MCMA+DD-MEKF can effectively improve the signal quality, compared to EGC+VVPE, optimized 1-2dB at both SER and MSE, and with higher tracking capability, can handle a larger range of line-width. Better signal quality is also shown on the constellation through reducing the impact of amplitude noise and phase noise. By using the AR algorithm, MEKF is updated to AKF, so that FSE-MCMA+DD-AKF can work under the 12kHz line-width that FSE-MCMA+DD-MEKF cannot reach, and the SER performance of FSE-MCMA+DD-AKF is 1-2dB better than that of FSE-MCMA+DD-MEKF. Better performance are all obtained under different conditions of atmospheric channel scintillation and wave-front distortion.

Based on the above, we propose a solution, by using adaptive fractionally-spaced blind equalization combined with adaptive kalman filter, under the minimum mean square error standard, the amplitude noise and phase noise are removed with the optimal bandwidth under time-varying conditions, so as to realize the phase synchronization of wireless coherent optical communication system in atmospheric channel. This method can be combined with spatial diversity in a natural way by fractionally-spaced equalization, so that the design not only uses the fusion of spatial diversity, but also has flexibility to make the system more adaptable to dynamic changes. Flexible phase synchronization can be more adaptable to future wireless optical network applications with dynamic, noisy, and diverse environments.

References

[1] M. Niu et al., "Performance analysis of coherent wireless optical communications with atmospheric turbulence," *Opt. Exp.*, vol. 20, no. 6, pp. 6515–6520, 2012, doi: 10.1364/OE.20.006515.

[2] G. Xu, Q. Zhang, Z. Song, and B. Ai, "Relay-assisted deep space optical communication system over coronal fading channels," *IEEE Trans. Aerosp. Electron. Syst.*, early access, Aug. 03, 2023, doi: 10.1109/TAES.2023.3301463.

[3] L. Qu, G. Xu, Z. Zeng, N. Zhang, and Q. Zhang, "UAV-assisted RF/FSO relay system for space-air-ground integrated network: A performance analysis," *IEEE Trans. Wireless Commun.*, vol. 21, no. 8, pp. 6211–6225, Aug. 2022, doi: 10.1109/TWC.2022.3147823.

[4] G. Xu and Q. Zhang, "Mixed RF/FSO deep space communication system under solar scintillation effect," *IEEE Trans. Aerosp. Electron. Syst.*, vol. 57, no. 5, pp. 3237–3251, Oct. 2021, doi: 10.1109/TAES.2021.3074130.

[5] G. P. Agrawal, *Fiber-Optic Communication Systems*. Hoboken, NJ, USA: Wiley, 2012.

[6] J. Vilà-Valls, M. Navarro, P. Closas, and M. Bertinelli, "Synchronization challenges in deep space communications," *IEEE Aerosp. Electron. Syst. Mag.*, vol. 34, no. 1, pp. 16–27, Jan. 2019, doi: 10.1109/MAES.2019.170208.

[7] M. Morelli and U. Mengali, "Feedforward frequency estimation for PSK: A tutorial review," *Eur. Trans. Telecommun.*, vol. 9, pp. 103–116, 1998, doi: 10.1002/ett.4460090203.

[8] J. Ma, K. Li, L. Tan, S. Yu, and Y. Cao, "Performance analysis of satellite-to-ground downlink coherent optical communications with spatial diversity over Gamma–Gamma atmospheric turbulence," *Appl. Opt.*, vol. 54, pp. 7575–7585, 2015, doi: 10.1364/AO.54.007575.

[9] A. Belmonte, A. Rodríguez, F. Dios, and A. Comerón, "Phase compensation considerations on coherent free-space laser communications system," *Proc. SPIE*, vol. 6736, 2007, Art. no. 67361A, doi: 10.1117/12.740276.

[10] P. Saxena, A. Mathur, and M. R. Bhatnagar, "BER performance of an optically pre-amplified FSO system under turbulence and pointing errors with ASE noise," *J. Opt. Commun. Netw.*, vol. 9, pp. 498–510, 2017, doi: 10.1364/JOCN.9.000498.

[11] Y. Fu et al., "BER performance analysis of coherent SIMO FSO systems over correlated non-kolmogorov turbulence fading with nonzero boresight pointing errors," *Opt. Commun.*, vol. 430, pp. 31–38, 2019, doi: 10.1016/j.optcom.2018.08.026.

[12] S. O. Zafra, X. Pang, G. Jacobsen, S. Popov, and S. Sergeyev, "Phase noise tolerance study in coherent optical circular QAM transmissions with Viterbi-Viterbi carrier phase estimation," *Opt. Exp.*, vol. 22, pp. 30579–30585, 2014.

[13] T. Pfau, S. Hoffmann, and R. Noé, "Hardware-efficient coherent digital receiver concept with feedforward carrier recovery for M-QAM constellations," *J. Lightw. Technol.*, vol. 27, no. 8, pp. 989–999, Apr. 2009, doi: 10.1109/JLT.2008.2010511.

[14] A. J. Viterbi and A. N. Viterbi, "Nonlinear estimation of PSK-modulated carrier phase with application to burst digital transmission," *IEEE Trans. Inf. Theory*, vol. 29, no. 4, pp. 543–551, Jul. 1983.

[15] X. Zhou, "Efficient clock and carrier recovery algorithms for single-carrier coherent optical systems: A systematic review on challenges and recent progress," *IEEE Signal Process. Mag.*, vol. 31, no. 2, pp. 35–45, Mar. 2014, doi: 10.1109/MSP.2013.2281071.

[16] L. Hongwei, H. Yongmei, W. Qiang, H. Dong, P. Zhenming, and L. Qing, "Phase offset tracking for free space Digital Coherent optical communication system," *Appl. Sci.*, vol. 9, no. 5, 2019, Art. no. 836, doi: 10.3390/app9050836.

[17] S. Jing and H. Puming, "Parallelized and adaptive square-root unscented Kalman filter for carrier recovery in satellite-to-ground coherent optical communications," *Opt. Commun.*, vol. 470, 2020, Art. no. 125697, doi: 10.1016/j.optcom.2020.125697.

[18] R. Mehra, "Approaches to adaptive filtering," *IEEE Trans. Autom. Control*, vol. 17, no. 5, pp. 693–698, Oct. 1972.

[19] Q. Zhang, Y. Yang, Q. Xiang, Q. He, Z. Zhou, and Y. Yao, "Noise adaptive Kalman filter for joint polarization tracking and channel equalization using cascaded covariance matching," *IEEE Photon. J.*, vol. 10, no. 1, Feb. 2018, Art. no. 7900911, doi: 10.1109/JPHOT.2018.2797050.

[20] P. R. Belanger, "Estimation of noise covariance matrices for a linear time-varying stochastic process," *Automatica*, vol. 10, no. 3, pp. 267–275, 1974.

[21] A. Almagbile, J. Wang, and W. Ding, "Evaluating the performances of adaptive Kalman filter methods in GPS/INS integration," *J. Glob. Positioning Syst.*, vol. 9, no. 1, pp. 33–40, 2010,.

[22] J. Surof, J. Poliak, and R. M. Calvo, "Demonstration of intradyne BPSK optical free-space transmission in representative atmospheric turbulence conditions for geostationary uplink channel," *Opt. Lett.*, vol. 42, pp. 2173–2176, 2017, doi: 10.1364/OL.42.002173.

[23] L. C. Andrews and R. L. Phillips, *Laser Beam Propagation Through Random Media*, 2nd ed. Bellingham, WA, USA: SPIE, 2005.

[24] X. Li, T. Geng, S. Ma, Y. Li, S. Gao, and Z. Wu, "Performance improvement of coherent free-space optical communication with quadrature phase-shift keying modulation using digital phase estimation," *Appl. Opt.*, vol. 56, pp. 4695–4701, 2017, doi: 10.1364/AO.56.004695.

[25] R. J. Noll, "Zernike polynomials and atmospheric turbulence," *J. Opt. Soc. Amer. A*, vol. 66, pp. 207–211, 1976.

[26] A. Belmonte and J. M. Khan, "Performance of synchronous optical receivers using atmospheric compensation techniques," *Opt. Exp.*, vol. 16, pp. 14151–14162, 2008, doi: 10.1364/OE.16.014151.

[27] C. R. Johnson, Jr. P. Schniter, I. Fijalkow, L. Tong, J. D. Behm, and M. G. Larimore, "The core of FSE-CMA behaviour theory," in *Unsupervised Adaptive Filtering*, vol. 2. Hoboken, NJ, USA: Wiley, 2000, pp. 1–17.

[28] J. Sun, P. Huang, Z. Yao, and J. Guo, "Adaptive digital combining for coherent free space optical communications with spatial diversity reception," *Opt. Commun.*, vol. 444, pp. 32–38, 2019, doi: 10.1016/j.optcom.2019.03.069.

[29] L. Pakala and B. Schmauss, "Extended Kalman filtering for simultaneous phase and amplitude noise mitigation in WDM systems," in *Proc IEEE 17th Int. Conf. Trans. Opt. Netw.*, 2015, pp. 1–4.

[30] K. N. Oh and Y. O. Chin, "Modified constant modulus algorithm: Blind equalization and carrier phase recovery algorithm," in *Proc. IEEE Int. Conf. Commun.*, 1995, pp. 498–502.

[31] B. D. O. Anderson and J. B. Moore, *Optimal Filtering*. Chelmsford, MA, USA: Courier Corporation, 2012.

[32] S. M. Kay, *Fundamentals of Statistical Signal Processing: Estimation Theory*. Hoboken, NJ, USA: Prentice-Hall, 1993.

[33] D. J. Geisler, T. M. Yarnall, M. L. Stevens, C. M. Schieler, B. S. Robinson, and S. A. Hamilton, "Multi-aperture digital coherent combining for free-space optical communication receivers," *Opt. Exp.*, vol. 24, pp. 12661–12671, 2016, doi: 10.1364/OE.24.012661.